International Journal of Applied Power Engineering (IJAPE)
Vol. 15, No. 2, June 2026, pp. 464~479
ISSN: 2252-8792, DOI: 10.11591/ijape.v15.i2.pp464-479

Super-twisting sliding mode control for enhanced performance of grid-connected PV systems with H-bridge multilevel inverter

CH. Venkata Amarnadh[1], T. Vijay Muni[1], T. Anuradha Devi[2], Rakesh Teerdala[3], M. Kiran Kumar[1], Kambhampati Venkata Govardhan Rao[3]
[1]Department of Electrical and Electronics Engineering, Koneru Lakshmaiah Education Foundation, Vaddeswaram, India
[2]Department of Electrical and Electronics Engineering, Vardhaman College of Engineering, Hyderabad, India
[3]Department of Electrical and Electronics Engineering, St. Martin's Engineering College, Secunderabad, India

Article Info

Article history:

Received Aug 18, 2025
Revised Dec 9, 2025
Accepted Jan 9, 2026

Keywords:

Direct model predictive control
Grid-connected PV system
Multilevel inverter
Super-twisting sliding mode control
Total harmonic distortion

ABSTRACT

This paper presents an enhanced control strategy for a grid-connected photovoltaic (PV) system employing a novel H-bridge multilevel inverter (MLI). The key contribution of this work lies in replacing the conventional proportional-integral (PI) controller with a super-twisting sliding mode controller (STSMC) for DC-link voltage regulation. Unlike earlier approaches that suffer from slow response, steady-state errors, and limited robustness under varying solar and temperature conditions, the proposed STSMC ensures faster transient response, finite-time convergence, and strong disturbance rejection without the chattering problem of classical sliding mode controllers. Another distinctive aspect of this study is the integration of STSMC with direct model predictive control (DMPC) for grid current regulation, enabling accurate reference current generation and improved synchronization. The novel H-bridge MLI topology further enhances system efficiency by reducing the number of switches while producing a seven-level output with lower total harmonic distortion (THD). Simulation results demonstrate that the proposed strategy achieves superior performance compared to the conventional PI-based system, with improvements in voltage stability, current quality, and reduced THD. These findings confirm the novelty and effectiveness of the proposed control scheme for reliable and efficient PV grid integration.

Corresponding Author:

Kambhampati Venkata Govardhan Rao
Department of Electrical and Electronics Engineering, St. Martin's Engineering College
Secunderabad, Telangana 500100, India
Email: kv.govardhanrao@gmail.com

1. INTRODUCTION

The worldwide shift toward renewable energy has notably driven the advancement of grid-connected photovoltaic systems [1]. Among the renewable technologies, photovoltaic (PV) systems are widely adopted due to their modularity, environmental friendliness, and steadily declining cost. A crucial challenge in these systems is the design of reliable and efficient power conversion and control strategies that can handle the nonlinear and time-varying nature of solar energy while ensuring stable power injection into grid [2]. Multilevel inverters (MLIs), especially those utilizing H-bridge configurations, are widely preferred in medium- and high-power systems due to their capability to produce high-quality output voltages with minimal total harmonic distortion (THD) and reduced voltage stress on power switches. The novel H-bridge multilevel inverter [3] topology further enhances system performance by reducing the number of switches required, thereby minimizing conduction losses, system complexity, and cost. This topology is particularly suitable for distributed generation systems that require efficient and scalable converter structures.

To achieve optimal performance in the system, a reliable control strategy is required that can maximize power extraction from the PV panels while maintaining grid current with low THD [4]. Direct model predictive control (DMPC) has recently emerged as a promising alternative to traditional control methods, offering advantages such as faster dynamic response, ease of handling multiple control objectives, and the capability to directly manipulate inverter switches without requiring a modulation stage. The existing methods employ DMPC for current control and a conventional proportional integral (PI) controller for DC-link voltage regulation [5].

Despite its widespread use owing to its simplicity and ease of integration, the PI controller has notable limitations, it suffers from several drawbacks in nonlinear and time-varying systems such as PV generation [6]. The limitations include slower response to abrupt changes in environmental conditions, steady-state errors under varying loads, and lack of robustness to disturbances. These issues become more prominent in PV systems where irradiance and temperature fluctuate rapidly, making it challenging for a linear controller to maintain accurate voltage tracking and ensure smooth power injection [7]. To overcome these limitations, this paper proposes an integration of a super-twisting sliding mode controller (STSMC) in place of the PI controller used in the original DMPC. The STSMC is a second-order sliding mode control strategy that confirms finite-time convergence, reduced chattering, and strong robustness against system uncertainties and external disturbances [8]. It effectively handles the nonlinearities of PV systems and enhances the regulation of DC-link voltages, which in turn improves the quality of the grid current reference generation [9], [10].

The proposed control strategy retains the DMPC for grid current control while modifying the reference current generation loop by introducing STSMC in the voltage control stage [11]. This integration leads to a more robust and adaptive control system that not only improves transient and steady-state performance but also ensures better tracking of maximum power point under dynamic operating conditions [12]. Furthermore, it contributes to the reduction of THD in the injected grid current and enhances power quality [13]. This paper offers detailed modeling and simulation of the enhanced control system. A comparative exploration between conventional PI controller and proposed STSMC-based scheme is conducted under various test conditions including step and ramp changes in irradiance and temperature [14]. The outcomes clearly validate superiority of proposed methods in terms of faster voltage regulation, reduced overshoot, improved current tracking, and lower THD. These findings confirm that the replacement of the PI controller with STSMC [15] significantly enhances the performance and reliability of system using H-bridge multilevel inverters [16].

2. LITERATURE SURVEY

Recent advancements in renewable energy control systems emphasize the limitations of conventional PI controllers, particularly their sensitivity to parameter variations and poor dynamic performance under non-linear conditions. In contrast, STSMC [17], a second-order sliding mode technique, has gained recognition for its robustness, finite-time convergence, and effective chattering suppression [18]. Various studies have demonstrated the superiority of STSMC in applications ranging from sensorless induction motor drives to standalone and grid-connected renewable systems [19]. Notably, the integration of STSMC with multilevel inverters (MLIs) enhances voltage regulation and reduces THD, thereby improving power quality. Additionally, recent multilevel inverter topologies aim to reduce the number of switching devices and eliminate the need for multiple DC sources, leading to simplified designs with high efficiency [20], [21]. These developments align well with the proposed control strategy in the manuscript, which leverages STSMC and an optimized H-bridge MLI for a grid-connected PV system [22], [23]. The combined approach not only ensures improved dynamic response and reliability under environmental disturbances [24], [25] but also meets modern grid compliance standards for renewable energy integration [26], [27]. Table 1 (see Appendix) gives the data of the literature survey [10], [12], [21], [22], [28]-[30].

3. SYSTEM MODELING

The system examined is a grid-connected PV setup featuring a new H-bridge MLI topology, illustrated in Figure 1. It is engineered to maximize power extraction from PV modules. That injects a high-quality current into the grid. The topology comprises three PV modules, two DC-link capacitors, a novel H-bridge multilevel inverter, an output filter, and a single-phase grid connection.

3.1. PV array and DC-link configuration

The PV source of the proposed system comprises three individual PV modules, denoted as PV1, PV2a, and PV2b. These modules are strategically arranged to form two distinct DC-links that supply the required voltage levels to the inverter. Specifically, PV1 forms the first DC-link on its own, while PV2a and PV2b are connected in series to constitute the second DC-link. This hybrid configuration enables the inverter to achieve multiple output voltage levels while minimizing the number of PV modules and associated power electronic components.

Each PV module is intended to operate at its individual maximum power point (MPP), which fluctuates based on environmental factors like sunlight intensity and temperature. Employing two independent DC-link configurations enables separate voltage regulation for each module, thereby improving the system's adaptability under partial shading or non-uniform operating conditions. The DC-link capacitors, denoted as C1 and C2, are connected across the outputs of PV1 and the series-connected PV2a–PV2b, respectively. These capacitors serve as energy buffers, smooth out voltage ripples, and provide a steady DC supply to inverters.

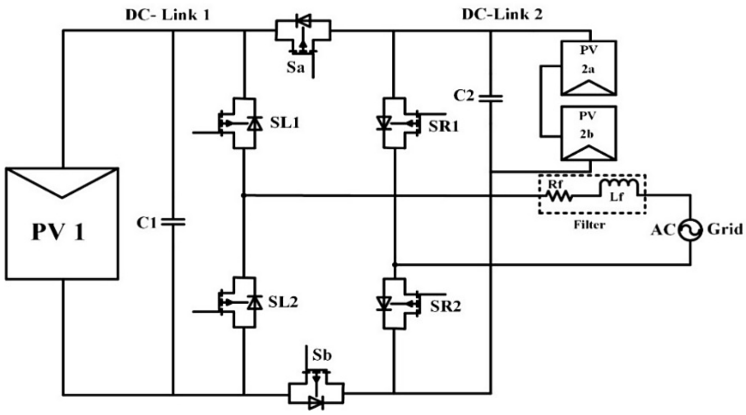

Figure 1. Proposed model of PV grid system

The rationale for connecting PV2a and PV2b in series is to achieve a higher voltage level $v_{\mathrm{pv2}} \approx 2v_{\mathrm{pv2}}$, which is essential for enabling the novel H-bridge inverter to synthesize seven distinct output voltage levels. These levels are $\{0, \pm v_{pv1}, \pm v_{pv2}, \pm(v_{pv1} + v_{pv2}\}$. This selective voltage generation improves the quality of the output waveform and reduces THD without requiring a larger number of switching devices or complex modulation techniques.

In addition to improving voltage resolution at the inverter output, the separate DC-link structure facilitates distributed MPPT control. This allows each DC-link to track its own MPP independently, even when different portions of the PV array experience varying levels of sunlight. The MPPT algorithm adjusts the reference $v_{pv1}^{*}$and v_{pv2}^{*}, which are later used in the voltage regulation loop to determine the required power injection into the grid.

The PV modules used in the simulation are modeled using standard I–V characteristics under varying conditions of solar. The system assumes that each module can deliver a nominal voltage of around 28.5 V and a current of 7.3 A at standard test conditions, as per the specifications. As PV2a and PV2b are in series, the second DC-link voltage approximately doubles, thus enabling the creation of higher output voltage steps in the multilevel inverter.

3.2. Novel H-bridge multilevel inverter

The power conversion unit in the proposed system is based on a modified H-bridge MLI topology. This inverter functions as the primary interface that links DC output from the PV modules to the AC utility grid. In contrast to traditional multilevel inverters that typically require numerous switching devices and multiple isolated DC sources, the adopted H-bridge configuration achieves seven-level voltage output with fewer semiconductor switches, offering a more compact and efficient design. This topology consists of six bidirectional switches (typically realized using MOSFETs), strategically configured to produce a mandatory multilevel voltage waveform. The voltage levels generated at the output terminal of the inverter are (1).

$$\{0, \pm v_{pv1}, \pm v_{pv2}, \pm(v_{pv1} + v_{pv2})\} \tag{1}$$

Here, v_{pv1} is the voltage across the first DC-link (from PV1), and v_{pv2} is the voltage through the second DC-link (from the series-connected PV2a and PV2b). The voltage magnitudes are selected such that $v_{pv2} \approx 2v_{pv1}$, enabling a wide range of output voltage combinations from a compact switching structure.

The key improvement of this topology lies in its capability to synthesize a staircase-like AC waveform that closely approximates a sine wave, using fewer switches compared to traditional cascaded H-bridge inverters. This reduction in switch count leads to lower conduction losses, reduced gate driver requirements, smaller heat sinks, and overall lower cost and complexity, without compromising the voltage level resolution or waveform quality.

Each switch in the inverter is capable of bidirectional current conduction and unidirectional voltage blocking, ensuring safe operation during different load and power flow conditions. The switching logic is derived from a predefined switching Table 2, which maps specific combinations of DC-link voltages to desired output voltage levels. This deterministic switching approach is particularly compatible with DMPC, which evaluates multiple switching scenarios in real time to optimize control performance.

The operation of the inverter can be briefly explained through the following example scenarios: i) When the output voltage needs to be zero, switching states are configured such that neither v_{pv1} nor v_{pv2} is connected to the output. To obtain $v_{out} = v_{pv1}$, the switches are arranged to apply only the first DC-link voltage; ii) Similarly, for $v_{out} = v_{pv1} + v_{pv2}$, both DC-links are coupled in series to the output; and iii) Negative voltage levels are generated by reversing the current path through appropriate switch selections.

This flexibility in voltage synthesis allows the inverter to closely track the sinusoidal reference current waveform, minimizing the THD and ensuring compliance with grid code standards. Additionally, the seven-voltage-level output waveform inherently improves the power quality and reduces the burden on the output filter components. In this system, the inverter works at a switching frequency determined by the DMPC algorithm, which evaluates a discrete-time model of the system and selects the optimal switching state at each sampling instant. This approach needs pulse-width modulation (PWM), further enhancing dynamic response and system efficiency.

Table 2. Switching patterns of the proposed H-bridge multilevel inverter

Index	Switching sequence			V_{out}
	SL1, SL2	SR1, SR2	Sa, sb	
1	0,1	0,1	1,0	$-(v_{pv1} + v_{pv2})$
2	0,1	1,0	0,1	v_{pv2}
3	0,1	1,0	1,0	-v_{pv1}
4	1,0	0,1	0,1	v_{pv1}
5	1,0	0,1	1,0	$-v_{pv2}$
6	1,0	1,0	0,1	$(v_{pv1} + v_{pv2})$
7	1,0	1,0	1,0	0

3.3. Grid-side filter and interface

A single-phase grid connection is established via an L-filter, consisting of an inductance L_f and a series resistance R_f. This filter attenuates high-frequency harmonics produced by inverter switching and helps maintain the quality of the current i_g injected into the grid, which is smooth and sinusoidal. The system does not employ a transformer, making it a transformerless configuration, which enhances efficiency and reduces size and cost. The grid voltage v_g is assumed to be a known and stable sinusoidal source. The inverter must inject a current in phase with this voltage to ensure unity power factor operation.

4. CONTROL STRATEGY

The control topology in the proposed grid-connected PV system is organized into three functional stages: MPPT, DC-link voltage regulation using STSMC, and grid current control DMPC. The complete block-level control flow, as implemented in Simulink, is illustrated in Figure 2.

In the first stage, two sets of PV modules (PV1 and PV2) are independently monitored, and their maximum power points are tracked using the perturb and observe (P&O) MPPT algorithm. Each PV module provides its respective voltage V_{pv1}, V_{pv2}, and current I_{pv1}, I_{pv2} to the MPPT blocks, which compute the optimal reference voltages V^*_{pv1} and V^*_{pv2} to extract maximum power. These reference voltages are compared with actual voltages to produce error signals for the voltage control stage.

The total MPP reference power is (2). This power is used to compute the ideal peak grid current under unity power factor conditions (3).

$$P^*_{total} = P^*_1 + P^*_2 \tag{2}$$

$$\hat{i}g = \frac{2P^*_{total}}{\hat{v}g} \tag{3}$$

The second stage incorporates the STSMC, which replaces the conventional PI controller. The STSMC receives the total DC-link voltage error $e = V_{pv}^{*} - V_{pv}$ and the previous error value e_{prev}, to generate a control output $u(t)$. This control signal regulates the peak reference value of grid current $\hat{I}$g. The actual instantaneous reference current I_g^{*} is then generated using $\hat{I}$g and the grid voltage V_g with the help of a phase-locked loop (PLL) to ensure synchronization with grid.

The combined DC-link voltage error is computed as (4). A sliding surface is defined as (5). It dynamically adjusts the reference current amplitude in (6).

$$e(t) = \left(v_{pv1} + v_{pv2}\right) - v_{pv1}^{*} + v_{pv2}^{*}) \tag{4}$$

$$s(t) = e(t) + \lambda \int e(t)dt \tag{5}$$

$$\hat{\imath}ga = \hat{\imath}g + u(t) \tag{6}$$

This corrected amplitude is used to generate the instantaneous sinusoidal reference current $i_g^{*}(t)$, ensuring stable power transfer and DC-link regulation. In the third stage, the DMPC controller utilizes the reference current I_g^{*}, measured grid current I_g, and predicted values $\hat{I}$g, V_{pv1}, V_{pv2} from a discrete prediction model. The controller evaluates a cost function over all feasible switching states to select the optimal control signals that minimize current and voltage tracking errors. These optimal states are used to drive switching devices of H-bridge inverter (SL1, SL2, SR1, SR2, Sa, Sb), enabling seven-level voltage synthesis for grid connection. A cost function is evaluated (7).

$$g = \lambda_i \left| i_g^{*} - i_g(k+1) \right| + \lambda_v \left(\left| v_{pv1}^{*} - v_{pv1}(k+1) \right| + \left| v_{pv2}^{*} - v_{pv2}(k+1) \right| \right) \tag{7}$$

The switching state that reduces the cost function is selected as the optimal choice by the DMPC controller. Based on this selection, the corresponding switching pattern is retrieved from the inverter's predefined switching table and used to generate the gating pulses for inverter switches. To enhance prediction accuracy, the system also incorporates a dedicated prediction block that estimates future values of key state variables such as grid current and PV voltages using current operating conditions. This feedforward prediction improves the controller's responsiveness and contributes to better dynamic stability, especially under fluctuating solar irradiance and temperature conditions. By switching the PI controller with the STSMC in the voltage regulation stage, the proposed control system achieves faster transient response, higher robustness to disturbances, and more accurate voltage tracking. These enhancements lead to improved quality in the reference current signal, resulting in significantly reduced THD in the grid current and overall better power quality in the grid-connected system. The parameter values of the system used for simulation and analysis are shortened in Table 3.

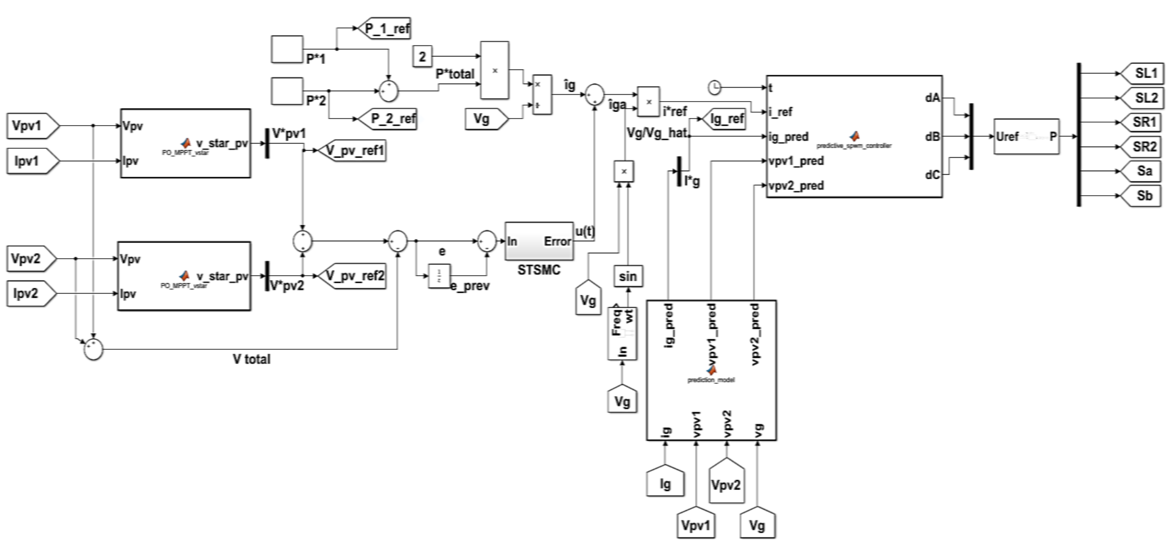

Figure 2. Controlling topology

Table 3. Parameter values of the system

Parameter	Symbol	Value
Cells per module	$Ncell$	60
Maximum power per module	Pmax	208.05
Open circuit voltage	Voc	36.3
Short circuit current	Isc	7.84
Voltage at maximum power point	Vmp	28.5
Current at maximum power point	Imp	7.3
DC link capacitors C1 and C2	-	47
Inductance	Lf2	5
Resistance	Rf2	10
Filter	Rf and Cf	5
Grid peak amplitude	AC grid	70
Switching frequency	fs	20
STSMC Gain 1	λ3	0.7
STSMC Gain 2	λ4	0.91

5. METHOD

The STSMC is a powerful control method designed to handle systems with uncertainties and external disturbances while ensuring strong stability. Traditional sliding mode control works by forcing the system's behavior onto a special surface called a sliding surface and keeping it there, which makes the system robust. However, this traditional method often causes a problem called chattering-rapid, unwanted switching in the control signal that can harm mechanical parts and reduce performance. STSMC solves this by using a second-order sliding mode technique that produces smooth, continuous control action, greatly reducing or eliminating chattering while maintaining the robustness of the system, as shown in Figure 3.

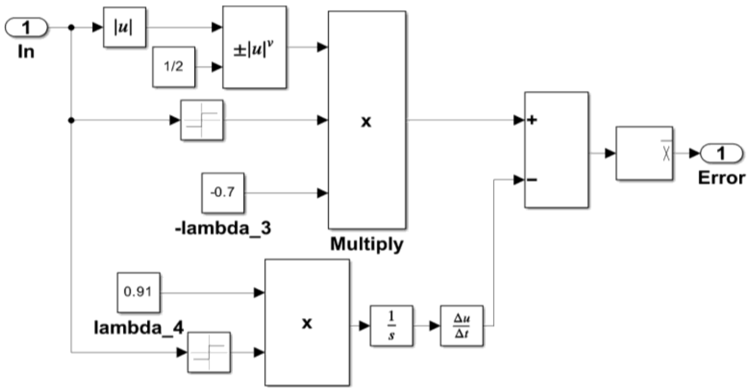

Figure 3. Control structure of the STSMC

STSMC achieves robust control by regulating both the sliding variable and its rate of change, enabling the system to reach the desired state quickly and accurately within a finite time. The controller employs a special control law composed of two parts: one that depends on the magnitude of the error, and another that adjusts based on the error's direction. This design ensures the system remains stable even in the occurrence of uncertainties and external disturbances, while providing smooth control and strong robustness. In this work, an improved control strategy is used for a novel H-bridge MLI. The key enhancement lies in replacing the conventional PI controller used for DC-link voltage regulation with the STSMC, overcoming limitations such as slow dynamic response and lack of robustness.

The STSMC structure is developed in simulation, as shown in Figure 3 model diagram. It receives DC-link voltage error (In), which represents the deviation between reference voltage and the actual aggregated PV voltage. The controller structure includes two main control terms: the super-twisting term and the integrator-based correction. The upper path of the diagram computes the first control component based on the square root of the absolute error multiplied by its sign. This term is then scaled by the gain $-\lambda_3 = -0.7$ and used to drive a fast corrective action for the tracking error. The lower path represents the second-order correction, where the error is multiplied by a gain $\lambda_4 = 0.91$ and then integrated over time to provide smooth and stable regulation.

The sum of these two control signals forms the final control action $u(t)$, which dynamically adjusts peak value of reference grid current. This value is passed to DMPC block, which uses it to compute the converting movements of the H-bridge inverter. The integration of STSMC enhances system's capability to reject disturbances and accurately track voltage references, even under rapidly changing solar conditions such as fluctuations in irradiance and temperature. Unlike traditional converters that rely on linear error correction and fixed gain tuning, STSMC offers nonlinear, robust control with finite-time convergence, making it well-suited for power electronic applications. In this project, implementing STSMC significantly improves the dynamic performance of DC-link voltage regulation. As a result, the quality of the generated reference current is enhanced, leading to lower THD in the grid current and better overall power quality on the grid side. The control gains for STSMC were carefully tuned through simulation to ensure stability and a fast dynamic response. The output of this controller dynamically adjusts reference current based on the voltage error, enabling the system to quickly respond to sudden disturbances or changes in operating conditions.

6. RESULTS AND DISCUSSION

To assess the effectiveness of the proposed STSMC combined with DMPC in a grid-connected PV system, extensive simulations were conducted using MATLAB/Simulink as displayed in Figure 4. The evaluation scenarios included changes in solar irradiance and temperature to analyze the system's dynamic behavior, voltage stability, power harvesting capability, and harmonic characteristics. The primary goal was to demonstrate that replacing the conventional PI controller with STSMC enhances the robustness, response time, and power quality of the system. Each simulation case studies a different disturbance scenario, and the system's behavior is analyzed through voltage, power, current, and THD responses.

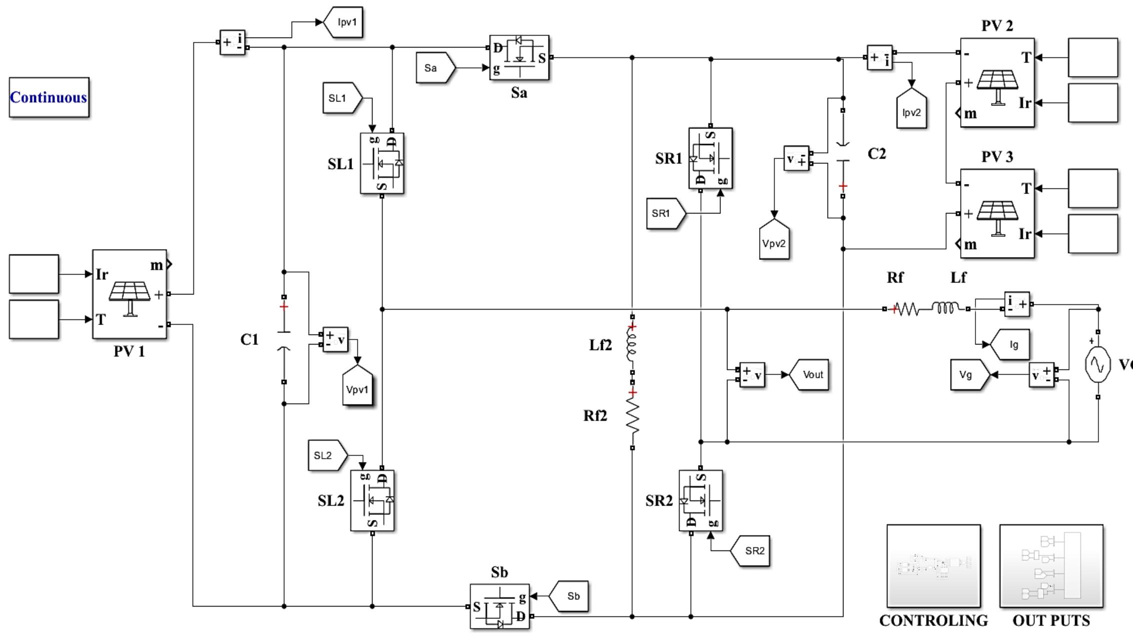

Figure 4. Simulation model of the proposed system

6.1. Case 1: Sudden variation in solar irradiance of PV1

Figure 5 illustrates the system response when the irradiance of PV1 is abruptly reduced from 1000 W/m² to 600 W/m². The reference voltage and power values adjust to the new irradiance, and the actual output accurately follows these references. The proposed STSMC demonstrates rapid tracking with negligible overshoot, in contrast to conventional PI controllers that typically exhibit lag and oscillatory behavior under such conditions. This confirms the effectiveness of STSMC in handling abrupt environmental variations, ensuring stable voltage regulation and continuous power injection into the grid.

6.2. Case 2: Step variation in solar irradiance of PV2a and PV2b

Figures 6 and 7 show the impact of step changes in irradiance on PV2a and PV2b. When irradiance drops in PV2a, the combined series-connected voltage rises while power output decreases. Similarly, PV2b exhibits corresponding voltage and power adjustments. The STSMC maintains smooth transitions with minimal ripple, while avoiding disturbance propagation to PV1 despite the shared DC-link. This highlights the controller's capability to isolate and stabilize the operation of multiple PV modules under partial shading conditions, ensuring independent maximum power point tracking for each DC-link.

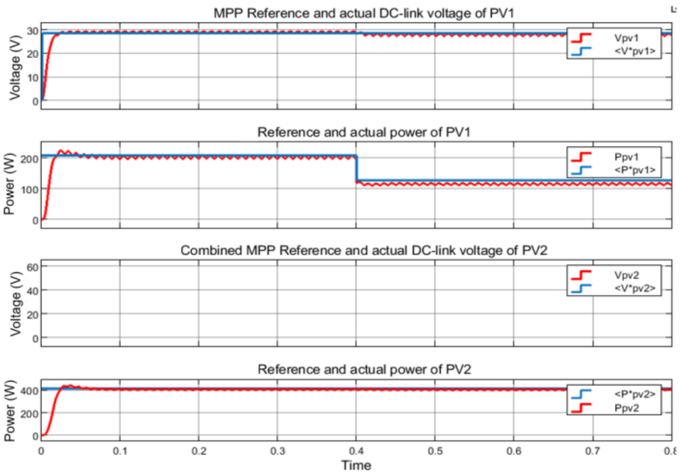

Figure 5. Simulation results of case 1

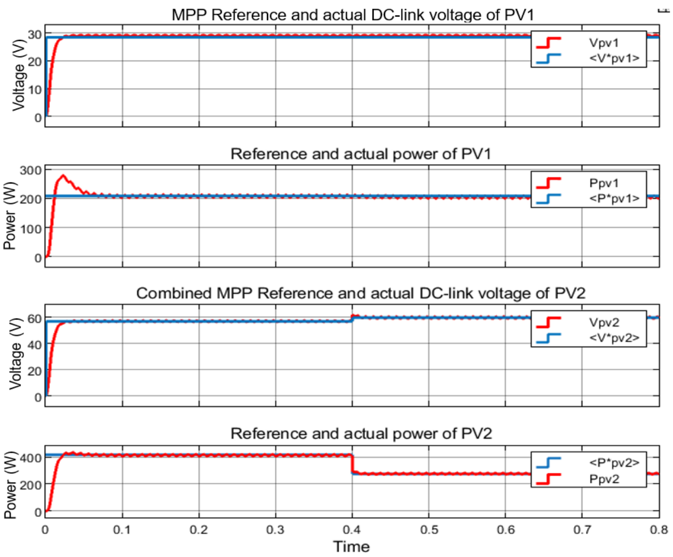

Figure 6. Variation of step in irradiance of PV2a

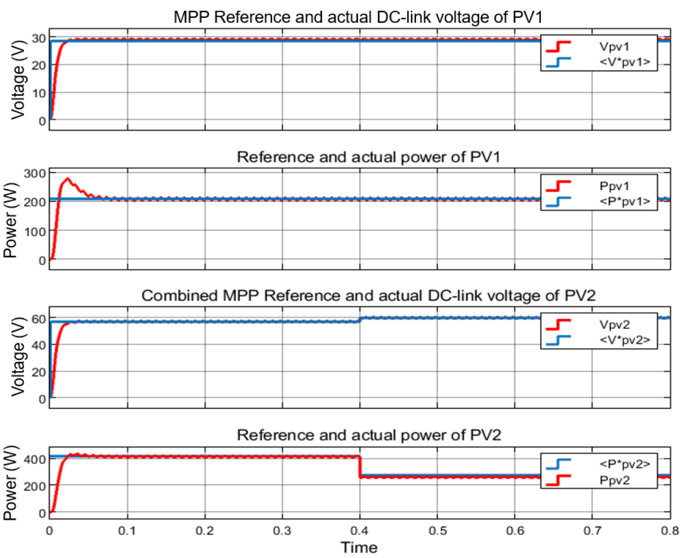

Figure 7. Step change in solar irradiance of PV2b

6.3. Case 3: Sudden variation in temperature of PV1

In Figure 8, the temperature of PV1 is increased from 25 °C to 35 °C at t = 0.4 s. The rise in temperature causes a drop in reference voltage and power, which the STSMC-controlled system tracks with high accuracy. Unlike PI controllers that often result in oscillations or delayed convergence under thermal disturbances, the STSMC maintains a stable response without ripple. This demonstrates its robustness against nonlinear temperature effects and its ability to preserve voltage stability under thermal stress.

6.4. Case 4: Sudden temperature variation of PV2a

Figure 9 shows the response when PV2a experiences a sudden temperature increase. The reference power decreases and the voltage slightly increases due to the thermal effect. The STSMC effectively tracks these changes with smooth and stable transitions. The absence of oscillations or delayed settling emphasizes the improved disturbance rejection of STSMC compared to conventional controllers, thereby validating its suitability for maintaining system stability during abrupt environmental fluctuations.

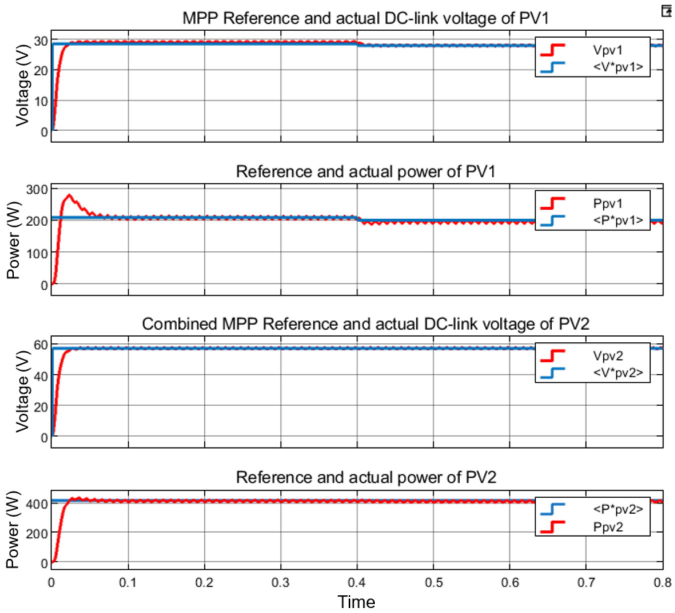

Figure 8. Simulation results of case 3

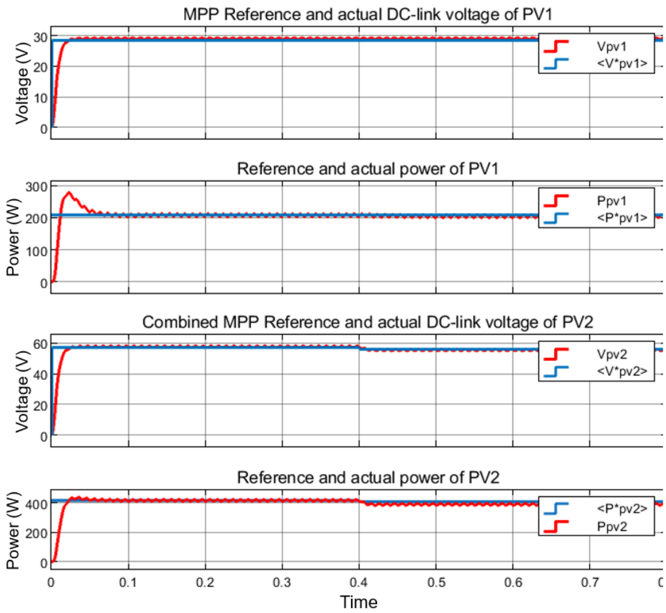

Figure 9. Simulation results of case 4

6.5. Case 5: Simultaneous variation in irradiance and temperature of PV1

Figure 10 demonstrates a compound disturbance where both irradiance and temperature of PV1 are varied simultaneously. This results in a sharp drop in output power and a moderate voltage change. Despite the combined nonlinear disturbances, the STSMC efficiently stabilizes both voltage and power with minimal deviation from reference values. The rapid and accurate regulation achieved under worst-case operating conditions confirms the superior adaptability of STSMC to real-world scenarios where multiple environmental parameters fluctuate concurrently.

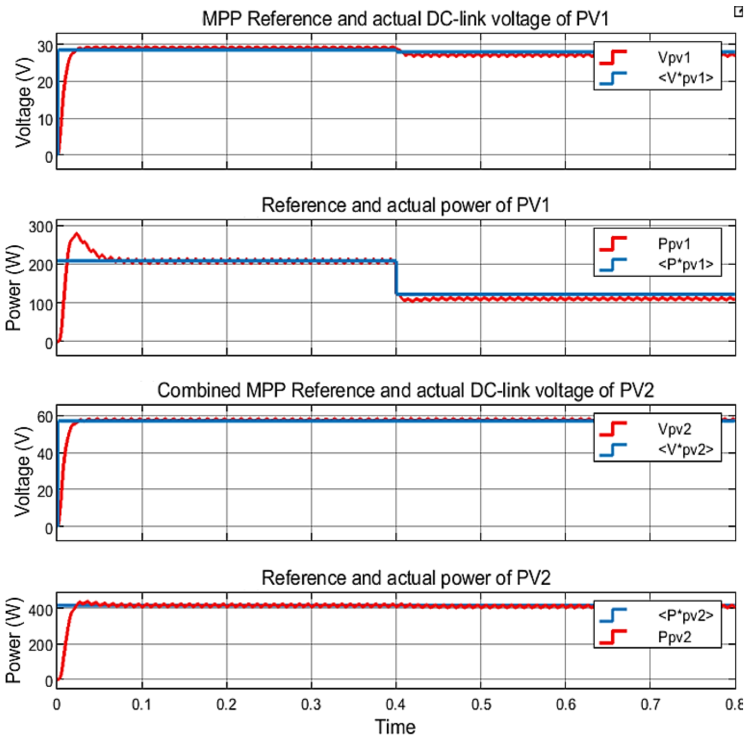

Figure 10. Step variation in irradiance and temperature of PV1

6.6. Case 6: Negative ramp change in irradiance of PV1

Figure 11 presents the effect of a gradual reduction in PV1 irradiance following a negative ramp function. The STSMC successfully manages this nonlinear and slow transition by maintaining accurate voltage and power tracking without lag or oscillations. In contrast, PI controllers typically exhibit delayed tracking under such conditions. This result demonstrates the adaptability of STSMC for handling real-life scenarios such as cloud movement and partial shading, where irradiance changes gradually rather than abruptly.

6.7. Case 7: Impact of step changes in solar irradiance on the grid current

Figure 12 illustrates the system performance in terms of grid current, grid voltage, and multilevel inverter output waveform during step irradiance changes. The actual grid current closely follows the reference, even under disturbances, and remains well synchronized with the grid voltage, ensuring operation at nearly unity power factor. The seven-level output waveform of the proposed inverter is clearly visible, demonstrating reduced harmonic content and better sinusoidal approximation compared to conventional topologies. This confirms the combined effectiveness of STSMC and DMPC in ensuring reliable grid synchronization and improved waveform quality.

6.8. Case 8: Power tracking under multiple disturbances

Figure 13 compares the reference maximum power point (MPP), extracted power, and delivered output power under a sequence of irradiance and temperature disturbances. The extracted and output power consistently track the reference values, demonstrating the ability of the proposed control scheme to sustain maximum power extraction and efficient energy transfer under dynamic conditions. This validates the coordination between STSMC and DMPC, where the STSMC ensures stable voltage regulation while DMPC guarantees accurate current tracking and grid injection.

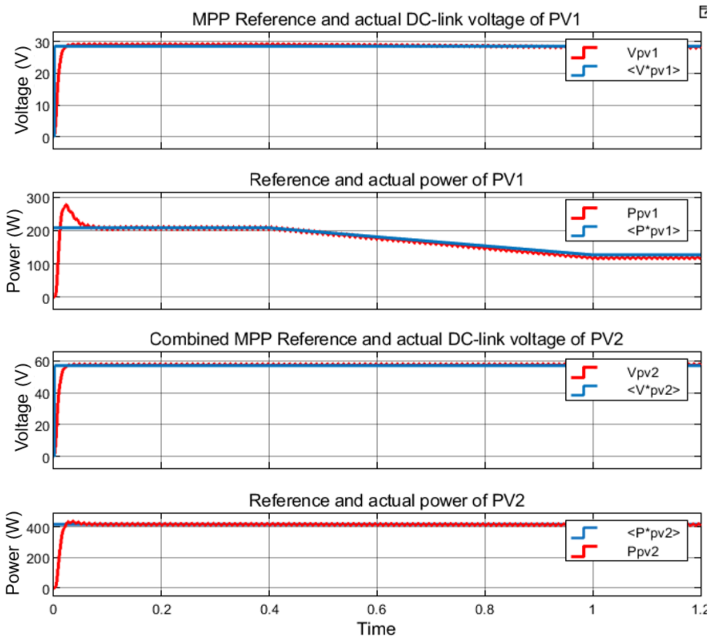

Figure 11. Effect of reduction in PV1 irradiance

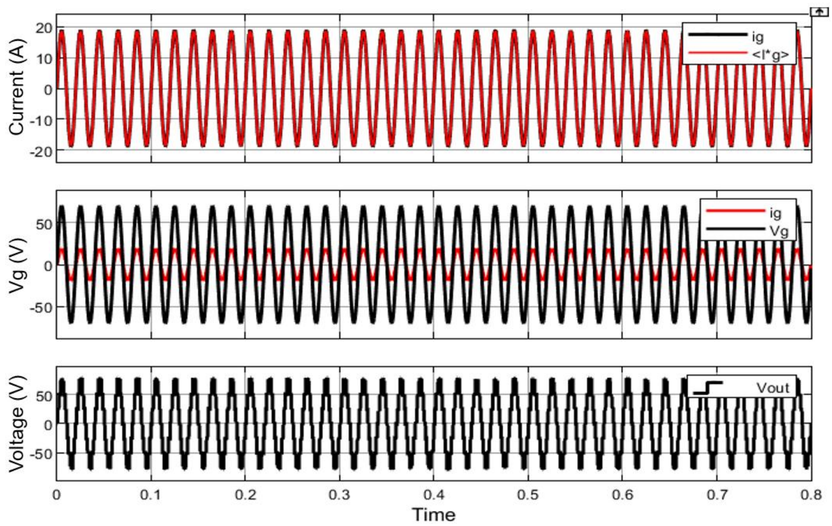

Figure 12. Grid current, grid voltage, and output voltage of multilevel inverter

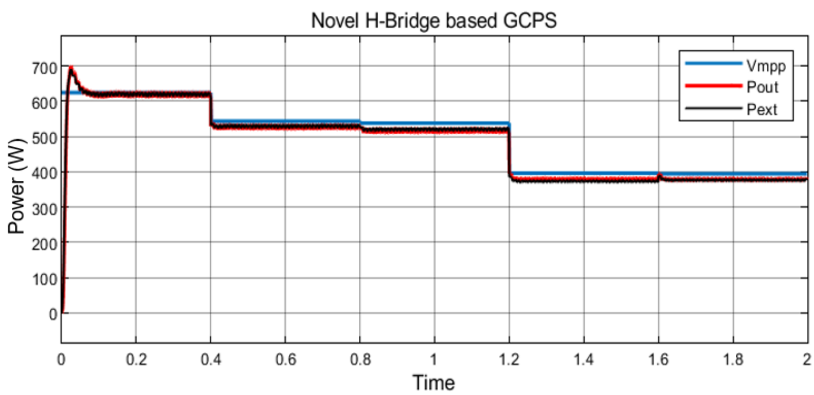

Figure 13. Comparison between powers

6.9. Case 9: THD analysis of both PI and STSMC

Figures 14 and 15, along with Table 4, present a comparison of THD performance between the conventional PI controller and the proposed STSMC. The grid current THD decreases from 2.56% with PI control to 2.01% with STSMC, representing an improvement of approximately 21.5%. Similarly, the output voltage THD reduces from 21.04% to 15.92%, a 24.3% improvement. These results confirm that the STSMC significantly enhances power quality by generating smoother reference currents and reducing inverter harmonics. The findings demonstrate the superiority of the proposed control strategy in meeting grid compliance standards and ensuring reliable PV grid integration.

The comparative results presented in Table 5 highlight the superior performance of the proposed STSMC over the conventional PI controller across various test scenarios. The STSMC demonstrated faster dynamic response, improved voltage and power tracking, and greater robustness under sudden changes in irradiance and temperature. Notably, it maintained better synchronization with the grid and achieved lower THD in both grid current and output voltage. These improvements confirm that integrating STSMC with DMPC significantly enhances the overall efficiency, power quality, and reliability of the grid-connected photovoltaic system.

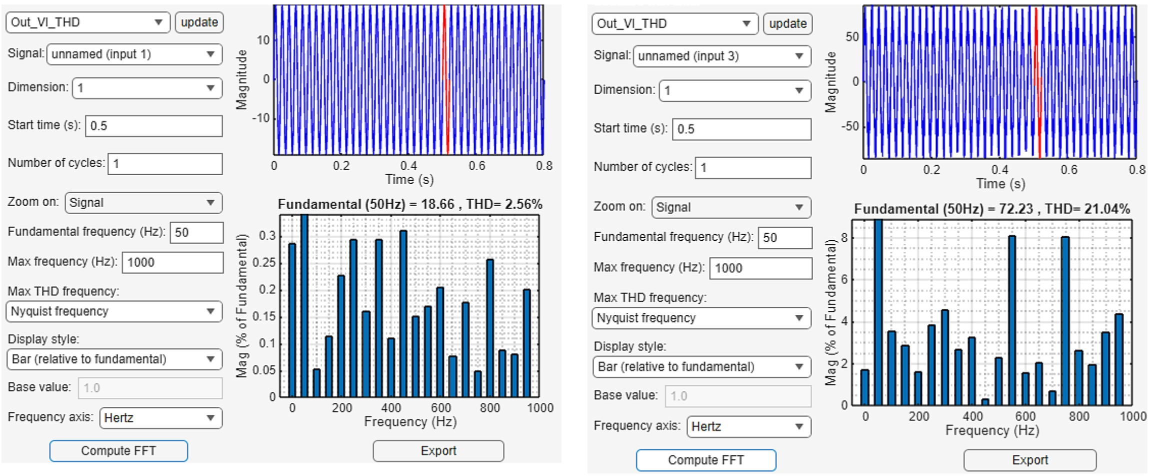

(a) (b)

Figure 14. THD percentage of the system with the PI controller: (a) grid current and (b) output voltage

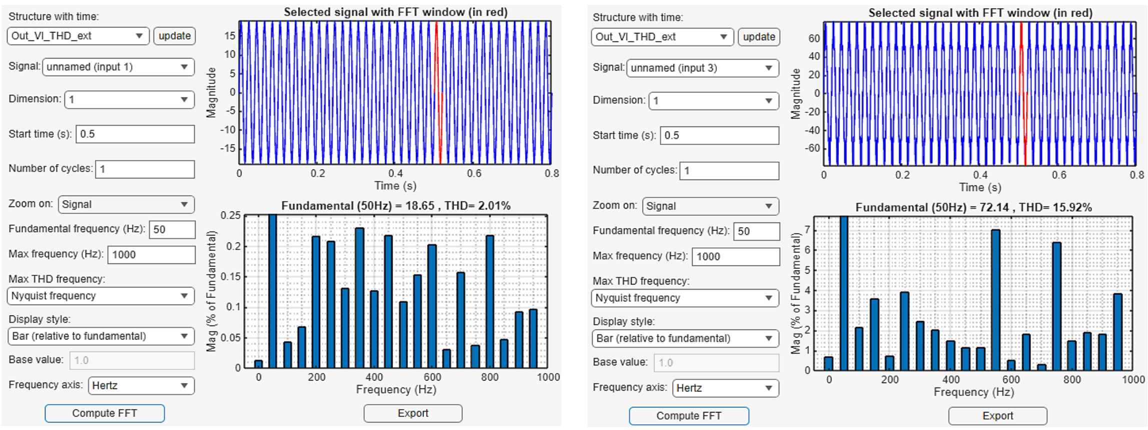

(a) (b)

Figure 15. THD percentage of the system with the ST-SMC controller: (a) grid current and (b) output voltage

Table 4. THD comparison

Parameter	PI controller	STSMC controller
Grid current THD	2.56	2.01
Output voltage THD	21.04	15.92

Table 5. Comparative table results and discussion

Test case	Observed parameter	PI controller	Proposed STSMC	Remarks
Case 1: Sudden drop in irradiance (PV1)	Voltage/power tracking	Slower tracking, small overshoot	Fast tracking, minimal overshoot	STSMC shows better dynamic response
Case 2: Step change in irradiance (PV2a, PV2b)	Voltage regulation	Moderate ripple, coupled disturbance	Smooth transition, isolated effect	Better control under partial shading
Case 3 and 4: Sudden temperature variation (PV1 and PV2a)	Thermal disturbance response	Voltage oscillations	Stable voltage	High thermal robustness of STSMC
Case 5: Simultaneous irradiance and temperature variation (PV1)	Voltage and power regulation	Delayed convergence	Fast and accurate regulation	Robust under compound disturbances
Case 6: Negative ramp in irradiance (PV1)	Smooth tracking	Lag in response	Accurate tracking	Better performance under gradual changes
Case 7: Grid synchronization	Grid current and voltage alignment	Slight misalignment	Excellent phase alignment	Better power factor and synchronization
Case 8: MPPT tracking under disturbances	Extracted vs reference power	Incomplete tracking	Accurate and continuous tracking	STSMC ensures MPPT even under fluctuations
Case 9: THD comparison	Grid current THD (%)	2.56	2.01	~21.5% improvement in grid current quality
	Output voltage THD (%)	21.04	15.92	~24.3% improvement in inverter voltage quality

7. CONCLUSION

This paper has presented an enhanced control strategy for a grid-connected photovoltaic (PV) system that integrates a novel H-bridge MLI with an STSMC and DMPC. The novelty of this work lies in replacing the conventional PI controller with STSMC for DC-link voltage regulation, enabling faster transient response, finite-time convergence, reduced chattering, and robust disturbance rejection under dynamic solar and temperature variations. In addition, the adoption of the proposed H-bridge MLI topology reduces the number of power switches while achieving a high-quality seven-level output, resulting in lower THD and improved power quality. Comparative simulations with PI-based control confirm the superior voltage regulation, better synchronization, and significant THD reduction achieved by the proposed method. While the results are promising, this study has certain limitations. The simulations were not extended to scenarios involving varying fault locations, unbalanced grid conditions, or different types of dynamic loads. Similarly, experimental validation was beyond the present scope and will be pursued in future work. These limitations open pathways for further research. Future work will focus on testing the proposed controller under fault ride-through conditions, integrating adaptive or intelligent control techniques to enhance real-time robustness, and extending the analysis to more complex multilevel inverter topologies and hybrid renewable systems.

FUNDING INFORMATION

Authors state no funding involved.

AUTHOR CONTRIBUTIONS STATEMENT

This journal uses the Contributor Roles Taxonomy (CRediT) to recognize individual author contributions, reduce authorship disputes, and facilitate collaboration.

Name of Author	C	M	So	Va	Fo	I	R	D	O	E	Vi	Su	P	Fu
CH. Venkata Amarnadh	✓	✓	✓	✓	✓	✓		✓	✓	✓			✓	
T. Vijay Muni		✓				✓		✓	✓	✓	✓	✓		
T. Anuradha Devi	✓	✓	✓	✓	✓	✓		✓	✓	✓			✓	
Rakesh Teerdala	✓		✓	✓			✓			✓	✓		✓	
M. Kiran Kumar	✓	✓	✓	✓	✓	✓		✓	✓	✓				
Kambhampati Venkata Govardhan Rao	✓		✓	✓			✓			✓	✓		✓	

C : **C**onceptualization
M : **M**ethodology
So : **So**ftware
Va : **Va**lidation
Fo : **Fo**rmal analysis
I : **I**nvestigation
R : **R**esources
D : **D**ata Curation
O : Writing - **O**riginal Draft
E : Writing - Review & **E**diting
Vi : **Vi**sualization
Su : **Su**pervision
P : **P**roject administration
Fu : **Fu**nding acquisition

CONFLICT OF INTEREST STATEMENT

Authors state no conflict of interest.

DATA AVAILABILITY

The authors confirm that the data supporting the findings of this study are available within the article.

REFERENCES

[1] B. Naima *et al.*, "Enhancing MPPT optimization with hybrid predictive control and adaptive P&O for better efficiency and power quality in PV systems," *Scientific Reports*, vol. 15, no. 1, 2025, doi: 10.1038/s41598-025-10335-0.

[2] I. Alia, I. Merzouk, M. M. Rezaoui, H. Rezk, and A. Lashab, "Output current observation and control of grid-connected modular multilevel converter using a simplified super twisting algorithm sliding mode," *Results in Engineering*, vol. 25, 2025, doi: 10.1016/j.rineng.2025.104280.

[3] H. G. Dirara, F. T. Yareshe, and C. M. Abdissa, "Design and analysis of adaptive fuzzy super-twisting sliding mode controller for uncertain 2-DOF robotic manipulator," *IEEE Access*, vol. 13, pp. 110241–110254, 2025, doi: 10.1109/ACCESS.2025.3581449.

[4] R. Tarkhani, S. Krim, M. Mansouri, and M. F. Mimouni, "Robust current sensor fault-tolerant controller using third order super-twisting sliding mode observer and controller for induction motors," *IEEE Access*, vol. 13, pp. 52841–52862, 2025, doi: 10.1109/ACCESS.2025.3553367.

[5] A. B. Djilali *et al.*, "Enhanced variable step sizes perturb and observe MPPT control to reduce energy loss in photovoltaic systems," *Scientific Reports*, vol. 15, no. 1, 2025, doi: 10.1038/s41598-025-95309-y.

[6] A. Sobh, B. Belabbas, and T. Allaoui, "Utilizing a five-level inverter for grid-connected PV systems: Implementing an MPPT algorithm with super twisting sliding mode control," *Przeglad Elektrotechniczny*, no. 8, pp. 210–214, 2024, doi: 10.15199/48.2024.08.43.

[7] M. Haghighat *et al.*, "Distributed power reserve control in grid-connected cascaded H-bridge converter-based photovoltaic systems," *IEEE Access*, vol. 12, pp. 168568–168580, 2024, doi: 10.1109/ACCESS.2024.3496518.

[8] M. A. B. Siddique, D. Zhao, A. U. Rehman, K. Ouahada, and H. Hamam, "An adapted model predictive control MPPT for validation of optimum GMPP tracking under partial shading conditions," *Scientific Reports*, vol. 14, no. 1, 2024, doi: 10.1038/s41598-024-59304-z.

[9] V. K. Dunna *et al.*, "Super-twisting MPPT control for grid-connected PV/battery system using higher order sliding mode observer," *Scientific Reports*, vol. 14, no. 1, 2024, doi: 10.1038/s41598-024-67083-w.

[10] A. Awadelseed, A. Lewicki, and A. Iqbal, "Single-phase 15-level switched-capacitor boost multilevel inverter topology for renewable energy applications," *IEEE Access*, vol. 12, pp. 90782–90793, 2024, doi: 10.1109/ACCESS.2024.3419265.

[11] O. T. Mahmood, W. Z. Wan Hasan, L. I. Ismail, H. R. H. Ramli, N. Azis, and N. M. H. Norsahperi, "Sliding mode controller optimization-based three-phase rectifier: review study," *IEEE Access*, vol. 12, pp. 101457–101483, 2024, doi: 10.1109/ACCESS.2024.3423776.

[12] K. V. G. Rao, A. D. Tellapati, T. V. S. Kalyani, R. M. Raj, J. Shanmugapriyan, and Y. Cooli, "Design of a temperature dependent industrial lighting," in *2025 5th International Conference on Trends in Material Science and Inventive Materials (ICTMIM)*, IEEE, Apr. 2025, pp. 730–734, doi: 10.1109/ICTMIM65579.2025.10988210.

[13] G. A. Ghazi *et al.*, "Circle search algorithm-based super twisting sliding mode control for MPPT of different commercial PV modules," *IEEE Access*, vol. 12, pp. 33109–33128, 2024, doi: 10.1109/ACCESS.2024.3372412.

[14] N. Debdouche, B. Deffaf, H. Benbouhenni, Z. Laid, and M. I. Mosaad, "Direct power control for three-level multifunctional voltage source inverter of PV systems using a simplified super-twisting algorithm," *Energies*, vol. 16, no. 10, 2023, doi: 10.3390/en16104103.

[15] W. Boucheritte, A. Moussi, R. Mechgoug, and H. Benguesmia, "A multilevel inverter for grid-connected photovoltaic systems optimized by genetic algorithm," *Engineering, Technology and Applied Science Research*, vol. 13, no. 2, pp. 10249–10254, 2023, doi: 10.48084/etasr.5558.

[16] J. Liu, Y. Yang, X. Li, K. Zhao, Z. Yi, and Z. Xin, "Improved model-free continuous super-twisting non-singular fast terminal sliding mode control of IPMSM," *IEEE Access*, vol. 11, pp. 85361–85373, 2023, doi: 10.1109/ACCESS.2023.3303843.

[17] X. Li, J. Liu, Y. Yin, and K. Zhao, "Improved super-twisting non-singular fast terminal sliding mode control of interior permanent magnet synchronous motor considering time-varying disturbance of the system," *IEEE Access*, vol. 11, pp. 17485–17496, 2023, doi: 10.1109/ACCESS.2023.3244190.

[18] F. Z. Khemili, O. Bouhali, M. Lefouili, L. Chaib, A. A. El-Fergany, and A. M. Agwa, "Design of cascaded multilevel inverter and enhanced MPPT method for large-scale photovoltaic system integration," *Sustainability (Switzerland)*, vol. 15, no. 12, 2023, doi: 10.3390/su15129633.

[19] K. V. G. Rao *et al.*, "A new brushless DC motor driving resonant pole inverter optimized for batteries," *International Journal of Power Electronics and Drive Systems*, vol. 14, no. 4, pp. 2021–2031, 2023, doi: 10.11591/ijpeds.v14.i4.pp2021-2031.

[20] S. Motahhir and A. Eltamaly, "Advanced Technologies for Solar Photovoltaics Energy Systems," *Green Energy and Technology*, 2021.

[21] B. Deffaf, F. Hamoudi, N. Debdouche, Y. Ayachi Amor, and S. Medjmadj, "Super-twisting sliding mode control for a multifunctional double stage grid-connected photovoltaic system," *Advances in Electrical and Electronic Engineering*, vol. 20, no. 3, pp. 240–249, 2022, doi: 10.15598/aeee.v20i3.4454.

[22] Y. Bendjeddou, A. Deboucha, L. Bentouhami, E. Merabet, and R. Abdessemed, "Super twisting sliding mode approach applied to voltage orientated control of a stand-alone induction generator," *Protection and Control of Modern Power Systems*, vol. 6, no. 1, p. 18, Dec. 2021, doi: 10.1186/s41601-021-00201-2.

[23] P. Gao, G. Zhang, H. Ouyang, and L. Mei, "An adaptive super twisting nonlinear fractional order PID sliding mode control of permanent magnet synchronous motor speed regulation system based on extended state observer," *IEEE Access*, vol. 8, pp. 53498–53510, 2020, doi: 10.1109/ACCESS.2020.2980390.

[24] K. V. G. Rao, M. K. Kumar, B. S. Goud, M. Bajaj, M. A. Houran, and S. Kamel, "Design of a bidirectional DC/DC converter for a hybrid electric drive system with dual-battery storing energy," *Frontiers in Energy Research*, vol. 10, Nov. 2022, doi: 10.3389/fenrg.2022.972089.

[25] A. I. Elsanabary, G. Konstantinou, S. Mekhilef, C. D. Townsend, M. Seyedmahmoudian, and A. Stojcevski, "Medium voltage large-scale grid-connected photovoltaic systems using cascaded H-bridge and modular multilevel converters: a review," *IEEE Access*, vol. 8, pp. 223686–223699, 2020, doi: 10.1109/ACCESS.2020.3044882.

[26] C. M. Abdissa and K. T. Chong, "Stabilization and voltage regulation of the Buck DC-DC converter using model predictive of Laguerre functions," *Studies in Informatics and Control*, vol. 26, no. 3, pp. 315–324, 2017, doi: 10.24846/v26i3y201707.

[27] F. T. Yareshe, N. W. Madebo, C. M. Abdissa, and L. N. Lemma, "Trajectory tracking of fixed-wing UAV using ANFIS-based sliding mode controller," *IEEE Access*, vol. 13, pp. 61986–62003, 2025, doi: 10.1109/ACCESS.2025.3557472.

[28] V. Patel, S. Di Gennaro, C. Buccella, and C. Cecati, "Super twisting sliding mode controller for PMSM fed with multilevel inverter for E-transportation," in *2020 IEEE 9th International Power Electronics and Motion Control Conference (IPEMC2020-ECCE Asia)*, IEEE, Nov. 2020, pp. 238–244, doi: 10.1109/IPEMC-ECCEAsia48364.2020.9368112.

[29] X. Zhu, S. Liu, and Y. Wang, "Second-order sliding-mode control of DFIG-based wind turbines," in *3rd Renewable Power Generation Conference (RPG 2014)*, Naples, 2014, pp. 1–6, doi: 10.1049/cp.2014.0936.

[30] A. Mousaei, M. B. B. Sharifian, and N. Rostami, "Direct thrust force control (DTFC) of optimized linear induction motor with super twisting sliding mode controller (STSMC)," in *2021 12th Power Electronics, Drive Systems, and Technologies Conference (PEDSTC)*, IEEE, Feb. 2021, pp. 1–5, doi: 10.1109/PEDSTC52094.2021.9405903.

APPENDIX

Table 1. Literature survey

Ref. No.	Focus area	Key contribution	Relevance to current work
[22]	Super twisting sliding mode control (STSMC) in wind energy systems	Proposed VFOC using STSMC for improved robustness and reduced harmonics in SEIG control	Demonstrates the superiority of STSMC over PI-based systems in renewable energy integration
[28]	PMSM control using STSMC with MLI	Shows enhanced drive performance and reduced chattering using STSMC with a 9-level inverter for E-transportation	Supports the use of STSMC with MLI for better control in power converters
[12]	Sensorless induction motor control	Introduced convergence-improved ST-SMO for better disturbance rejection and speed estimation	Reinforces the robustness of STSMC in dynamic and uncertain environments
[10]	Switched capacitor multilevel inverter (SC-MLI)	Developed a 15-level isolated SC-MLI with high gain and reduced switch count	Highlights the design advantages of low-component, high-performance MLI topology
[29]	2nd order sliding mode control in wind turbines	Used the super-twisting algorithm to control both RSC and GSC, improving dynamic response and robustness	Confirms STSMC suitability for grid-tied renewable systems with dual converters
[30]	STSMC for electric drives	Compared STSMC with classical SMC, showing reduced chattering and faster convergence	Validates STSMC as an advanced control method for high-precision applications
[21]	Stand-alone induction generator with STSMC	Proposed STSMC with SVM for reduced harmonics and improved voltage control	Demonstrates STSMC's adaptability across different renewable energy applications

BIOGRAPHIES OF AUTHORS

CH. Venkata Amarnadh was born in Repalle, Andhra Pradesh, India. He received the B.Tech. degree in electrical and electronics engineering (first class with distinction) in 2023 from Narasaraopeta Engineering College, affiliated to JNTU Kakinada, Guntur, Andhra Pradesh, India. He is currently studying as a PG student in the EEE department, Koneru Lakshmaiah Education Foundation (KL Deemed to be University). His research interests include electric vehicles and power systems. He can be contacted at email: chennupalliamarnadh2000@gmail.com.

Dr. T. Vijay Muni is an assistant professor and researcher with more than 13 years of experience in the Department of Electrical and Electronics Engineering at KL Deemed to be University. He received his B.Tech. degree in electrical and electronics engineering from JNTU Hyderabad, M.Tech. degree in power system and industrial drives from JNTUK, Kakinada, and a doctoral degree from KL Deemed to be University. He has authored 5 textbooks on electrical discipline. He has published over 52 Scopus-indexed articles, 12 Web of Science-indexed articles, and over 15 articles in peer-reviewed journals, and also published 6 patents with two grants. His areas of research include power electronic converters, energy management systems, control of electric power grids, renewable energy systems, and microgrids. He is an active senior member of IEEE. He can be contacted at email: vijaymuni1986@gmail.com.

Dr. T. Anuradha Devi is working as an associate professor in the Department of EEE, Vardhaman College of Engineering, Hyderabad. She received her Ph.D. in electrical drives from the KLU Andhra Pradesh. She received M.Tech. degree with the specialization in power electronics and electric drives from JNTU Hyderabad, and a B.Tech. degree in electrical and electronics engineering from Nagarjuna University, A.P. She has published more than 35 research papers in reputed international conferences, journals, and book chapters. She also published more than 10 patents. She has 10 years of experience in teaching. Her research interests include electric vehicle drives and powertrain optimization, power electronics for sustainable energy systems, switched reluctance motor (SRM) control, multilevel and DC-DC converter topologies, smart grid and microgrid technologies, and energy storage with battery management. She also focuses on applying artificial intelligence and machine learning techniques to power electronics and advanced electric drive systems. She can be contacted at email: anuradhadevi.eee@gmail.com.

Rakesh Teerdala is an associate professor in the Electrical and Electronics Engineering Department at St. Martin's Engineering College. He earned his Ph.D. in power systems from Jawaharlal Nehru Technological University-Hyderabad in 2018. He completed his M.Tech. in electrical power systems from the same renowned institution in 2011. His educational journey began with a bachelor's degree in electrical and electronics engineering from ADAMS Engineering College, Paloncha, in 2009. He has a teaching career spanning 14 years, his research interests encompass a wide range of topics, including FACTS controllers, power electronics applications to power systems. His contributions include 2 Indian patent publications, 2 textbooks, and 27 national/international journals and conferences. He can be contacted at email: santoshikanagala@gmail.com.

Dr. M. Kiran Kumar is working as an associate professor in the Department of Electrical and Electronics Engineering Koneru Lakshmaiah Education Foundation (KL Deemed to be University) College of Engineering, and has about 16 years of teaching experience. He received his B.Tech. degree in electrical and electronics engineering with distinction from JNTU Hyderabad and M.E. degree in power electronics and drives with distinction from Anna University, Chennai. He received Ph.D. degree in electrical and electronics engineering from KL Deemed to be University, Guntur, Andhra Pradesh. He has published more than 70 Scopus, SCI, and ESCI research papers in refereed international journals and 16 research papers in the proceedings of various international conferences and three patents in his credit. He received the Best Teacher Award five times, and his research interests include switched reluctance machines, power electronics, electric vehicles, and control systems. He is an active member of SIEEE, MISTE, and IEI. He can be contacted at email: kiran.malligunta@gmail.com.

Kambhampati Venkata Govardhan Rao is currently working as an assistant professor in Electrical and Electronics Engineering Department, St. Martin's Engineering College, Dhulapally, Secunderabad, Telangana. He holds Doctor of Philosophy degree from Koneru Lakshmaiah Educational Foundation (KL Deemed to be University), Vijayawada Campus. He completed his Master of Technology at Abdul Kalam Institute of Technological Sciences, Vepalagadda, Kothagudem, affiliated to JNTU Hyderabad, and Bachelor of Technology at Abdul Kalam Institute of Technological Sciences, Vepalagadda, Kothagudem, affiliated to JNTU Hyderabad. He has more than 9 years of teaching experience. He published over 25 papers in various reputed journals, attended 10 conferences with ISBN number along with 4 best paper awards, and published 6 Indian patents. He guides 5 M.Tech. students and 18 B.Tech. students. He is also a life member in Indian Society for Technical Education and Indian Association for Engineers. His areas of research include power electronics, power systems, converters, and electric vehicles. He can be contacted at email: kv.govardhanrao@gmail.com.